CORA Cork Open Research Archive
Cartlann Taighde Oscailte Chorcaí

Title	A study of the temperature dependence of the local ferroelectric properties of c-axis oriented Bi6Ti3Fe2O18 Aurivillius phase thin films: Illustrating the potential of a novel lead-free perovskite material for high density memory applications
Authors	Faraz, Ahmad;Deepak, Nitin;Schmidt, Michael;Pemble, Martyn E.;Keeney, Lynette
Publication date	2015-08-07
Original Citation	Faraz, A., Deepak, N., Schmidt, M., Pemble, M. E. and Keeney, L. (2015) 'A study of the temperature dependence of the local ferroelectric properties of c-axis oriented Bi6Ti3Fe2O18 Aurivillius phase thin films: Illustrating the potential of a novel lead-free perovskite material for high density memory applications', AIP Advances, 5(8), 087123 (14 pp). doi: 10.1063/1.4928495
Type of publication	Article (peer-reviewed)
Link to publisher's version	http://scitation.aip.org/content/aip/journal/adva/5/8/10.1063/1.4928495 - 10.1063/1.4928495
Rights	© 2015 Author(s). All article content, except where otherwise noted, is licensed under a Creative Commons Attribution 3.0 Unported License. - https://creativecommons.org/licenses/by/3.0/
Download date	2025-01-28 12:36:08
Item downloaded from	https://hdl.handle.net/10468/7699

UCC
University College Cork, Ireland
Coláiste na hOllscoile Corcaigh

AIP Advances

A study of the temperature dependence of the local ferroelectric properties of c-axis oriented Bi6Ti3Fe2O18 Aurivillius phase thin films: Illustrating the potential of a novel lead-free perovskite material for high density memory applications

Ahmad Faraz, Nitin Deepak, Michael Schmidt, Martyn E. Pemble, and Lynette Keeney

Citation: AIP Advances **5**, 087123 (2015); doi: 10.1063/1.4928495
View online: http://dx.doi.org/10.1063/1.4928495
View Table of Contents: http://scitation.aip.org/content/aip/journal/adva/5/8?ver=pdfcov
Published by the AIP Publishing

Articles you may be interested in

Macroscopic and nanoscale electrical properties of pulsed laser deposited (100) epitaxial lead-free Na 0.5 Bi 0.5 TiO 3 thin films
J. Appl. Phys. **107**, 034102 (2010); 10.1063/1.3290956

Ferromagnetic, ferroelectric, and fatigue behavior of (111)-oriented BiFeO 3 / (Bi 1 / 2 Na 1 / 2) TiO 3 lead-free bilayered thin films
Appl. Phys. Lett. **94**, 172906 (2009); 10.1063/1.3127519

Piezoresponse and ferroelectric properties of lead-free [Bi 0.5 (Na 0.7 K 0.2 Li 0.1) 0.5] Ti O 3 thin films by pulsed laser deposition
Appl. Phys. Lett. **92**, 222909 (2008); 10.1063/1.2938364

High piezoelectric response in polar-axis-oriented Ca Bi 4 Ti 4 O 15 ferroelectric thin films
Appl. Phys. Lett. **85**, 3519 (2004); 10.1063/1.1807010

Uniform field-induced strain in a/b -axes-oriented Bi 3.9 Pr 0.1 Ti 3 O 12 thick films on IrO 2/Si substrates for lead-free piezoelectric microdevice applications
Appl. Phys. Lett. **85**, 1220 (2004); 10.1063/1.1783020

All article content, except where otherwise noted, is licensed under a Creative Commons Attribution 3.0 Unported license. See: http://creativecommons.org/licenses/by/3.0/ Downloaded to IP: 143.239.65.133 On: Tue, 15 Sep 2015 07:37:49

AIP ADVANCES **5**, 087123 (2015)

A study of the temperature dependence of the local ferroelectric properties of *c*-axis oriented $Bi_6Ti_3Fe_2O_{18}$ Aurivillius phase thin films: Illustrating the potential of a novel lead-free perovskite material for high density memory applications

Ahmad Faraz,[1,a] Nitin Deepak,[1] Michael Schmidt,[1] Martyn E. Pemble,[1,2] and Lynette Keeney[1]
[1]*Tyndall National Institute, University College Cork, 'Lee Maltings', Dyke Parade, Cork, Ireland*
[2]*Department of Chemistry, University College Cork, Cork, Ireland*

(Received 3 October 2014; accepted 20 July 2015; published online 7 August 2015)

The ability to control the growth, texture and orientation of self-nanostructured lead-free Aurivillius phase thin films can in principle, greatly improve their ferroelectric properties, since in these materials the polarization direction is dependent on crystallite orientation. Here, we report the growth of *c*-plane oriented $Bi_6Ti_3Fe_2O_{18}$ (B6TFO) functional oxide Aurivillius phase thin films on *c*-plane sapphire substrates by liquid injection chemical vapour deposition (LI-CVD). Microstructural analysis reveals that B6TFO thin films annealed at 850°C are highly crystalline, well textured (Lotgering factor of 0.962) and single phase. Typical Aurivillius plate-like morphology with an average film thickness of 110nm and roughness 24nm was observed. The potential of B6TFO for use as a material in lead-free piezoelectric and ferroelectric data storage applications was explored by investigating local electromechanical (piezoelectric) and ferroelectric properties at the nano-scale. Vertical and lateral piezoresponse force microscopy (PFM) reveals stronger in-plane polarization due to the controlled growth of the *a*-axis oriented grains lying in the plane of the B6TFO films. Switching spectroscopy PFM (SS-PFM) hysteresis loops obtained at higher temperatures (up to 200°C) and at room temperature reveal a clear ferroelectric signature with only minor changes in piezoresponse observed with increasing temperature. Ferroelectric domain patterns were written at 200°C using PFM lithography. Hysteresis loops generated inside the poled regions at room and higher temperatures show a significant increase in piezoresponse due to alignment of the *c*-axis polarization components under the external electric field. No observable change in written domain patterns was observed after 20hrs of PFM scanning at 200°C, confirming that B6TFO retains polarization over this finite period of time. These studies demonstrate the potential of B6TFO thin films for use in piezoelectric applications at elevated temperatures and for use in non-volatile ferroelectric memory applications. © *2015 Author(s). All article content, except where otherwise noted, is licensed under a Creative Commons Attribution 3.0 Unported License.* [http://dx.doi.org/10.1063/1.4928495]

I. INTRODUCTION

Ferroelectric materials are a valuable class of materials whose dipole moments can be switched by application of an electric field at room and higher temperatures and which remain in the switched state even when the field is removed.[1] Ferroelectric materials may also be associated with other

[a]ahmad.faraz@tyndall.ie

 ©Author(s) 2015

All article content, except where otherwise noted, is licensed under a Creative Commons Attribution 3.0 Unported license. See: http://creativecommons.org/licenses/by/3.0/ Downloaded to IP: 143.239.65.133 On: Tue, 15 Sep 2015 07:37:49

physical properties such as piezoelectricity, pyroelectricity, high optical activity and non-linear dielectrics etc.[2,3] Such physical properties are effectively utilized in ferroelectric random access memories (Fe-RAMs), sensing and actuating applications.[4,1,5]

Among these multifunctional ferroelectric oxides, the lead-based perovskite, $Pb(Zr,Ti)O_3$ (PZT) and PZT-based multicomponent systems (ceramics and thin films) are widely used in data storage devices (Fe-RAMs), sensors, micro actuators, transducers, capacitors and in the microelectronic industries due to their superior piezoelectric properties (d_{33} 200 pC/N) compared with other oxide systems.[5] However, due to the volatile nature of lead and vaporization of lead oxides during processing at high temperature, lead products are subject to serious toxicological and environmental concerns. In Europe, two different legislations were passed relating to 'Waste from Electrical and Electronic Equipment (WEEE)' and 'Restriction of Hazardous Substances (RoHS)'.[6,7] According to these legislations, lead and other hazardous substances used in electric and electronic products are restricted and the manufacturer of these products will be responsible for recycling of lead based components. These restrictions are imposed on 10 different categories of electronics and electrical equipment which include small and large house hold appliances, IT (information technology) and telecommunications equipment, lighting equipment, consumer, toys leisure, monitoring and control, automatic dispensers and medical equipment.[8] While these restrictions are not currently affecting the piezoelectric industry due to the difficulty in finding convenient comparable substituents with effectively reduced environmental impact and high piezoelectric coefficients (d_{33}) to replace lead, it is however known thatlead-based materials with lead contents of 60% and above will be banned in the near future.[9]

Consequently, toxicity, volatility, high temperature instability and evaporation of lead in lead-based materials motivates the quest for developing novel lead free piezoelectric materials with potentially high temperature stabilities and advanced electromechanical/piezoelectric properties.[10,11] The origin of piezoelectricity in PZT-based perovskites is a result of the intrinsic structural non-centrosymmetry and lone pair Pb^{2+} electrons effectively contributing to spin exchange energy in hybrid orbitals.[12,13] Furthermore, non-centrosymmetric phases formed near the morphotropic phase boundary (MPB) demonstrate enhanced piezoelectric properties. Due to similarities in the electronic structures of Pb^{2+} and Bi^{3+} and their typically high Curie temperatures (T_c generally over 500°C) and stabilities, Bi^{3+} based systems are considered as potential candidates to replace lead in multicomponent piezoelectric systems, especially for elevated temperature applications such as automotive engine sensors and high temperature Fe-RAMs.[3,14]

To date, an extensively studied and scientifically interesting family of bismuth-based piezoelectrics is the bismuth layer-structured ferroelectric (BLSF) family in the Aurivillius phase.[15–18] Aurivillius phase materials are naturally 2-*D* nanostructured, consisting of $(Bi_2O_2)^{2+}$ blocks interleaved with alternating $nABO_3$ perovskite units (where *n* ranges from *2-9*), described by the general formula Bi_2O_2 ($A_{n-1}B_nO_{3n+1}$), where *A* represents differing cations with valence states ranging from +1 to +3 such as monovalent Na^+, K^+, divalent Ca^{2+}, Mg^{2+}, Sr^{2+}, Pb^{2+}, Ba^{2+} and trivalent Zr^{3+}, Yt^{3+} etc. *B* represents cations with valence states ranging from +3 to +5 such as Fe, Mn, Ti, Nb etc. and *n* represents the number of perovskite units per half unit cell. In the perovskite unit cell A-site cations are coordinated to 12 oxygen ions and lie at the corner of the cell whereas B-site cations are located at the centre of the cell and coordinate to 6 oxygen ions.[15,17]

The diversity of intrinsic structural tuning, variation in the number of perovskite blocks (*n*) and the flexibility to accommodate wide varieties of *A* and *B*-site cations within the perovskite units (in consideration of the structural tolerance factor (T_f)) allow for tailoring of properties, such as the multiferrioc properties,[17] the reduction of leakage currents and polarization switching fatigue.[17,18] For instance, $SrBi_2Ta_2O_9$ ($n = 2$) and $Bi_{3.25}La_{0.75}Ti_3O_{12}$ ($n = 3$) have been commercially developed for use in Fe-RAMS due to their reduced switching fatigue and high temperature stabilities as compared to lead ziroconate titanate (PZT) based materials.[19–21]

It is well-know that bismuth layer structured Arivilius phase thin films (BLSF) with odd-numbers of perovskite units show spontaneous polarization (P_s) along the in-plane *a*-axis and minor polarization along the out-of-plane *c*-axis, while even *n*-numbered films demonstrate response along the out-of-plane *a*-axis only.[22,35] Ferroelectric polarization in these materials is strongly hindered by additional impurity phases (such as pyrochlore).[23] These microstructural defects can be

All article content, except where otherwise noted, is licensed under a Creative Commons Attribution 3.0 Unported license. See: http://creativecommons.org/licenses/by/3.0/ Downloaded to IP: 143.239.65.133 On: Tue, 15 Sep 2015 07:37:49

overcome by using optimised growth processes. For instance, the deposition of highly textured, oriented and uniform thin films can in principle extensively improve desired physical properties such as ferroelectric polarization, in material systems where the polarization is dependent on crystal orientation. Aurivillius phase materials have been previously fabricated in both bulk and thin film form using molten solid state reaction (MSS),[24] sol-gel[10] and pulse laser deposition (PLD) processes,[25] however, to date no report is available on deposition of $n = 5$ layer $Bi_6Ti_3Fe_2O_{15}$ thin films using liquid injection chemical vapour deposition (LI-CVD). This is a pulsed liquid injection technique in which the volume and injection rate of precursor is controlled electronically in microliter (μL) and pulse per milliseconds (pulse/msec). This technique allows high growth rates of low vapour pressure multicomponent precursors (e.g. bismuth $(thd)_3$) in thin film form for high-*k* dielectrics and ferroelectric applications with high uniformity and control of thickness, orientation, texture and composition.[22]

In this paper, we report the growth of *c*-axis oriented $Bi_6Ti_3Fe_2O_{15}$ ($n = 5$) Aurivillius phase thin films on *c*-plane oriented sapphire substrates using the horizontal flow liquid injection chemical vapour deposition (LI-CVD) method. The potential of B6TFO for high temperature applications such as high temperature ferroelectric random access memories (Fe-RAMs) was explored at the nano-scale by analysing local piezoelectric and ferroelectric phenomena (domain switching, polarization writing and reading of patterns etc.) using piezoresponse force microscopy (PFM) measurements as a function of temperature applied in-situ. Fine polarizations patterns (100-300nm) were written and read at elevated temperature (200°C) and the stability of these patterns with respect to time (>20hrs) is illustrated.

II. EXPERIMENTAL

$Bi_6Ti_3Fe_2O_{18}$ (B6TFO) thin films were grown by a liquid injection chemical vapour deposition (lI-CVD) technique using a horizontal flow Aixtron AIX 200/FE AVD (atomic vapour deposition) reactor equipped with a pulsed liquid delivery injection setup. In this system liquid precursors are injected into the Trijet vapourizer in mixture form. Low vapour pressure precursors were transferred onto *c*-plane oriented single side polished sapphire (2inch diameter and 430μm thick) substrates using N_2 as carrier gas. Sapphire substrates were cleaned with isopropyl alcohol (IPA), dried with nitrogen and loaded into the reaction chamber which was rotated at 60rpm over a susceptor to obtain uniform depositions (observed average roughness for B6TFO was 24nm). Commercially available (SAFC-Hitech) liquid organometallic precursors $Bi(thd)_3$ (thd = 2,2,6,6-tetramethyl-3,5-heptanedionate), $Fe(thd)_3$, and $Ti(O\text{-}iPr)_2(thd)_2$ (O-iPr = iso-propoxide) dissolved in toluene were used at concentrations of 0.1 M. The ratios of net volumetric precursor injection delivery were kept at 7.5:3:2 for $Bi(thd)_3$ (thd = 2,2,6,6-tetramethyl-3,5-heptanedionate), $Ti(O\text{-}iPr)_2(thd)_2$ and $Fe(thd)_3$, respectively by adjusting the pulse frequency and injection time during the growth run. The net volumetric precursor ratios transferred in vapour form into the reaction vapourizer (Trijet) are controlled by a computer controlled system operated at 220°C. Due to the low deposition efficiency and volatile nature of bismuth at higher temperatures, 25% excess was added to compensate any bismuth deficiencies and to suppress the formation of mixed and pyrochlore phases during the annealing phase, as is well reported in literature for MOCVD (metal organic chemical vapour deposition) processes.[22,26] A liquid flow meter was used to monitor the net liquid flow during processing. The deposition temperature and pressure were kept at 610°C and 10 mbar, respectively, while O_2 was used as a reactant gas with a flow rate of 600sccm (standard-state cubic centimetre per minute). Fabricated films were annealed in a conventional commercial furnace at varied set temperatures in the range 800-900°C to investigate the optimum temperature for crystallisation of single phase B6TFO. X-ray diffraction (XRD) patterns were collected over the range $5 \leq 2\Theta \leq 40°$ at room temperature using a Philips Xpert PW3719 MPD diffractometer equipped with a Cu-Kα radiation source (operating at 45kV and 40mA) and nickel filter. XRD data was used to investigate the degree of orientation of B6TFO thin films by calculating the Lotgering factor (LF) by comparing the ratios of peaks along the preferred orientation to summation of all diffracted intensities peak and using theoretical (hkl) intensities obtained from the Crystallographica software.[26–28]

All article content, except where otherwise noted, is licensed under a Creative Commons Attribution 3.0 Unported license. See: http://creativecommons.org/licenses/by/3.0/ Downloaded to IP: 143.239.65.133 On: Tue, 15 Sep 2015 07:37:49

Microstructure, morphology and topography were examined using high resolution transmission electron microscopy (HR-TEM Jeol 2100, 200 kV, double tilt holder), high resolution scanning electron microscopy (FEI Nova 630 HR-SEM) and atomic force microscopy (MFP-3D Asylum Research AFM in AC mode using Olympus AC160TS silicon cantilevers (Al reflex coated, <300 kHz resonance frequency)). For TEM (transmission electron microscopy) analysis, cross-sections of the B6TFO thin films were prepared using a FEI Helios Nanolab Focus ion beam (FIB) with final thinning achieved at 93PA 30kV and polishing at 2kV 28PA. The *d*-spacing along the preferred *c*-axis was calculated using the selected area diffraction (SAED) mode. Local electromechanical properties such as electromechanical switching, in-plane and out of plane piezoresponses and ferroelectric polarization induced patterning at room and high temperature were investigated using a piezoresponse force microscopy (PFM) system equipped with a high voltage amplifier HVA220 (MFP-3D Asylum Research). In-plane and out-of-plane electromechanical responses were analyzed by single frequency PFM[29] using an electrilever operating at a frequency (20 kHz) lower than the tip/sample contact resonance cantilever frequency.[30] Amplified out-of-plane electromechanical responses were measured by dual AC resonance tracking piezoresponse force microscopy (DART-PFM) using the electrilever close to the tip/sample contact resonance frequency and by tracking the resonance frequency to minimize topography cross-talk.[30] Olympus AC240TM Electrilevers, Ti/Pt coated silicon cantilevers (Al reflex coated, 70 kHz resonant frequency, ~320 kHz contact resonance frequency) were used for PFM imaging. In order to calibrate the cantilever before imaging the sample surface, the inverse optical lever sensitivity (InvOLs) was calibrated for each new cantilever according to the MFP-3D procedural manualette. Domain patterns were introduced ('written') onto the sample surface and 'read' using the Asylum Research PFM lithography mode using an applied DC bias (Vdc) higher than the ferroelectric coercive field (H_c) of the sample.

III. RESULTS AND DISCUSSION

A. Crystallographic Properties

The crystal structure of the B6TFO thin films deposited onto *c*-plane sapphire substrates was investigated using X-Ray diffraction (XRD) and high resolution transmission electron microscopy (HR-TEM) as illustrated in figures1 and 2. In order to determine the most favorable temperature to achieve optimum crystallinity of single phase $Bi_6Ti_3Fe_2O_{18}$, B6TFO thin film samples were annealed at different temperatures over the range 800°C-900°C. XRD patterns (figure1 a-b) reveal that preferential orientation of the B6TFO thin films is along the *c*-axis and crystallinity increases with an increase in annealing temperature. Peaks designated with asterisk (*) are from the sapphire substrate and the XRD sample holder. To visualize and identify possible impurities and secondary phases, the x-ray intensity data was plotted in a logarithmic scale. The observed XRD peaks were indexed on the basis of relevant layered structured Aurivillius phase profiles, (Joint committee on powder diffraction (JCPDS No. 38-1257) sapphire substrate and CuKβ peaks.

B6TFO films annealed at 850°C for 10min illustrated in figure1(a) exhibit reflections consistent with an $n = 5$ Aurivillius phase structure with average lattice parameters $a = 5.47$, $b = 5.38$ and $c = 49.26$ Å. No additional impurity or secondary phases such as the spinel structures (the most prominent peak is expected at 35.4° for the (311) reflection) or pyrochlore phases (the most prominent peak is expected at 29.96° for the (444) reflection) were detected in scan in range $5 \leq 2\Theta \leq 40°$. However, it should be noted that background noise level during XRD scanning limits the detectability of such minor phases. Minor secondary phases with trace level volumes below 3 vol% of the parent composition are typically undetectable by the XRD technique.[17] Although previous investigations of the $Bi_5Ti_3Fe_{0.7}Co_{0.3}O_{15}$ thin films demonstrated that trace levels of magnetic spinel impurities can significantly contribute to magnetic responses observed in oxide thin films,[17,31] the presence of these minor phases at trace level would not be expected to influence the overall ferroelectric response of films showing uniform piezoresponse to any significant degree. XRD peaks become sharper and the FWHM (full width at half maxima) values decrease (the FWHM of the (0012) peak decreases from 0.37°-0.25°)) with respect to increase in temperature (800°C- 900°C),

All article content, except where otherwise noted, is licensed under a Creative Commons Attribution 3.0 Unported license. See: http://creativecommons.org/licenses/by/3.0/ Downloaded to IP: 143.239.65.133 On: Tue, 15 Sep 2015 07:37:49

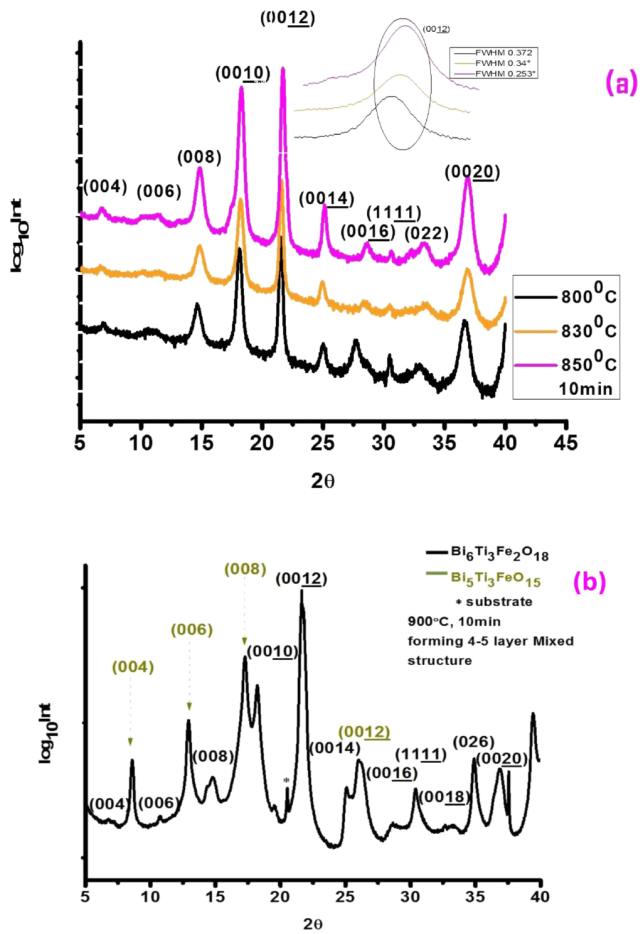

FIG. 1. X-ray diffraction patterns representing the effect of temperature on crystallinity and phase formation for $B6Ti_3Fe_2O_{18}$ thin films on c-plane sapphire substrates: (a) 800ºC, 830ºC, 850ºC (b) a mixed phase Aurivillius material demonstrating intergrowths of a 4 ($Bi_5Ti_3FeO_{15}$) and 5 ($Bi_6Ti_3Fe_2O_{18}$) -layered phase was observed for thin films annealed at 900ºC. The reflections labelled in black font are from the 5-layered phase while those labelled in green font are from the 4-layered phase.

confirming an increase in crystallinity. Additional XRD peaks were observed for B6TFO when annealing conditions were increased to 900C° for 10min as illustrated in figure1(b). These additional peaks were attributed to reflections of a mixed layered Aurivillius phase structure having both $n = 5$ and $n = 4$ repeating units within the sample. Such mixed layer phases may be attributed due to volatility, instability and evaporation of Bi at higher annealing temperatures.[15] Since ferroelectric polarization is influenced by the degree of orientation and texture of Aurivillius phase films, the degree of orientation for the B6TFO films is expressed in terms of Lotgering factor.[27] The Lotgering factor (L_f) measured for the B6TFO thin film annealed at 850^0C was 0.962, confirming that the B6TFO thin film is preferably oriented along the out-of-plane c-axis (c-plane) and textured[27,28] although full texture was not obtained (L_f<1) as observed by the (11$\underline{1}$1) and (026) reflections.

Figure 2 represents a cross-section HR-TEM micrograph of a B6TFO thin film annealed at 850°C. TEM analysis reveals that the B6TFO thin film has a clear n = 5 layered Aurivillius structure with uniformly distributed perovskite units over the sample. The average unit cell length of 4.8 nm along the c-axis is in good agreement with the observed XRD results. No intergrowth and impurity phases with differing unit cells parameters were observed by TEM analysis.

B. Morphology and composition

High resolution scanning electron microscopy (HRSEM) micrographs represented in figure3(a)-3(b) at high and low magnification reveals that B6TFO (annealed at 850°C, 10min) thin films exhibit

All article content, except where otherwise noted, is licensed under a Creative Commons Attribution 3.0 Unported license. See: http://creativecommons.org/licenses/by/3.0/ Downloaded to IP: 143.239.65.133 On: Tue, 15 Sep 2015 07:37:49

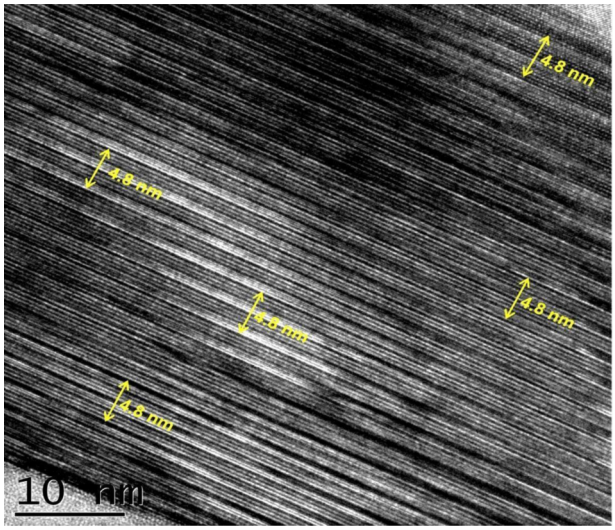

FIG. 2. Microstructural analysis: representative HRTEM cross-section image of an Aurivillius phase B6Ti3Fe2O18 sample on c-plane sapphire annealed at 850°C for 10min.

grains crystallized with plate-like morphology which is characteristic of the layered structure Aurivillius phase materials. Furthermore, SEM-EDX ratios confirm the stoichiometry of the $Bi_6Ti_3Fe_2O_{18}$ composition. Due to the layered nature of the B6TFO crystals, the thickness varied across the film. An average thickness, measured using cross-section SEM for B6TFO thin film (850°C, 10min) was 110nm as represented in figure 3(b).

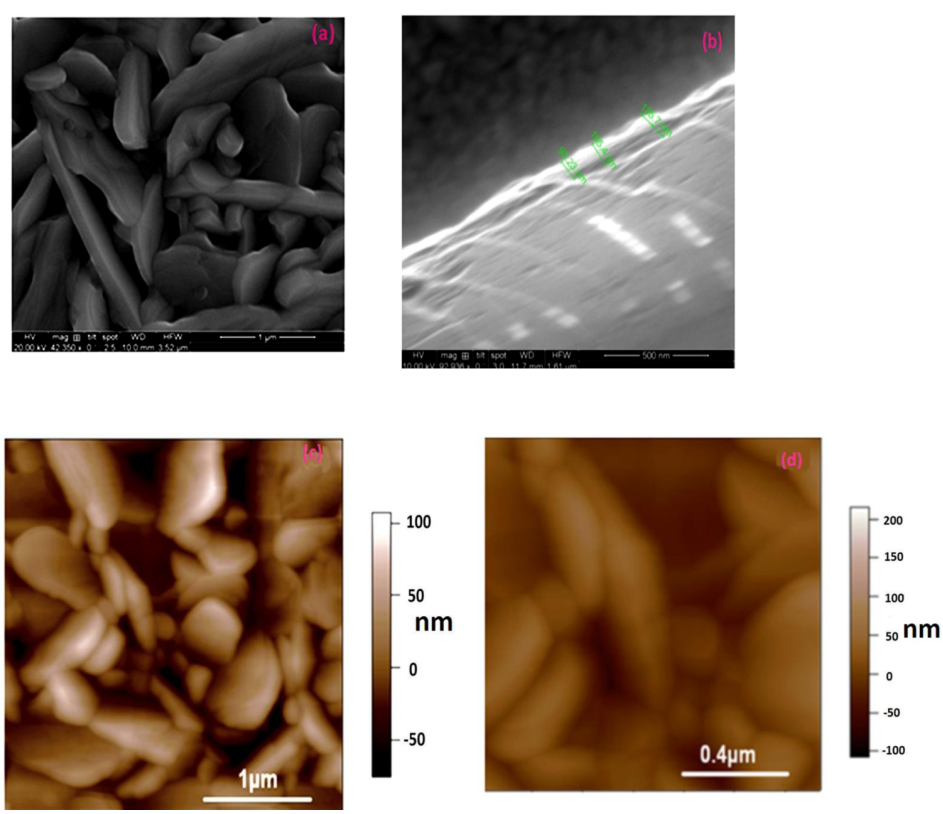

FIG. 3. Representative (a) HR-SEM top-view (b) HR-SEM cross-section (c) and (d) AFM topography images of $B_6Ti_3Fe_2O_{18}$ thin films.

All article content, except where otherwise noted, is licensed under a Creative Commons Attribution 3.0 Unported license. See: http://creativecommons.org/licenses/by/3.0/ Downloaded to IP: 143.239.65.133 On: Tue, 15 Sep 2015 07:37:49

The surface topography of the B6TFO thin film is illustrated in figure 3(c)-3(d), as imaged by AFM. The plate-like morphology is also evident by AFM and the average surface roughness for the B6TFO thin films annealed at 850°C for 10 minutes is estimated to be ca. 24nm.

Since, Pyrochlore phase strongly influences ferroelectric/piezoelectric properties of Aurivilius phase thin films. STEM with EDX provides capabilities to perform local elemental mapping to scrutinize Bi6Ti3Fe2O18 thin film samples for possible investigation of secondary phase inclusions. The elemental mappings were conducted over 51x44 μm2 over 72hrs scan time as illustrated in fig. 4. From these EDX elemental mappings, it can be seen that there is clear evidence of 1 Fe rich area of 0.2x0.5x3.8μm. HR-TEM was performed over this region to investigate n perovskite units as illustrated in inset of fig.4(b). More interestingly, it was observed that Fe rich phase has same bismuth content as primary main phase for 5-layer Aurivilius phase structure. Only the slight Ti content was lowered by the amount of Fe increment in perovskite unit of Aurivilius structure. The ratios on Fe access over the Ti content at B-site of perovskite unit was further investigated by performing various number of point EDX spectra over this region as illustrated in Fig. 4(f). The net observed average Ti: Fe in this region was 2.8: 2.2 and average variation in composition was Bi3Ti2.8Fe2.2O18. While observed average major primary composition for main phase in Bi6Ti3Fe2O18. This excess in Fe content may be introduced in primary phase due to inappropriate mixing during LI-CVD growth.

C. Local electromechanical and ferroelectric polarization

The potential of B6TFO thin films for use in high density data storage ferroelectric devices (FeRAMs) at elevated temperature (in our case 200°C) was investigated at the local level by visualizing the ferroelectric polarization associated with domain structure, domain switching, polarization reversal, writing and reading multi-domain patterns (by aligning polarization along one direction). Piezoresponse force microscopy (PFM) is a powerful non-destructive tool and the dual AC resonance tracking (DART), vertical piezoresponse force microscopy (VPFM), lateral piezoresponse force microscopy (LPFM) and lithography modes[29,30,32,34] were used to analyse the associated physical properties at elevated temperature (up to 200°C) at the local submicron/nano scale.

1. Local in-plane and out-of-plane electromechanical and ferroelectric polarization investigations

The magnitude of ferroelectric polarization and polar orientation within the plane and out-of-plane was investigated by scanning B6TFO samples in the lateral and vertical single frequency PFM modes, respectively to investigate the suitability of B6TFO thin film for in-plane or out-of-plane memory switching applications. In this mode, topographical cross-talk from sample grains is avoided by scanning the sample at a lower frequency (20 kHz) than the cantilever contact resonance frequency (300-310 kHz) (figure 5(a)-5(d)). It is well established that the magnitude of ferroelectric polarization (P_s) in layered Aurivillius phase structures is influenced by the number of perovskite units (n).[22] As noted earlier, Aurivillius phases with odd numbers of perovskite units have their spontaneous polarization vector along the in-plane a-axes and show weak or minor out-of-plane c-axis polarization (P_s), while Aurivillius phases with even numbers of perovskite units (n) show spontaneous response along in-plane a-axis polarization.[22,35] The amplitude response observed at room temperature demonstrates that the B6TFO films are piezoelectric, with comparably higher ferroelectric polarization strength and piezoresponses in the lateral a-axis direction (figure 5(b)) with those measured in the vertical direction (figure 4(a)). Phase responses as illustrated in figure5(c)-5(d) along the vertical out-of-plane and lateral in-plane directions, respectively, demonstrate naturally self-polarized piezoelectric domains with preferential orientation either along 0° or 180° with respect to the PFM tip. The differences between the topography and natural self-polarized domains are easily observable by comparing figures 5(a)-5(e). These results demonstrate that the increased ferroelectric polarization strength along the lateral plane compared with the vertical plane indicates a preference for B6TFO for possible use in in-plane switching devices.

All article content, except where otherwise noted, is licensed under a Creative Commons Attribution 3.0 Unported license. See: http://creativecommons.org/licenses/by/3.0/ Downloaded to IP: 143.239.65.133 On: Tue, 15 Sep 2015 07:37:49

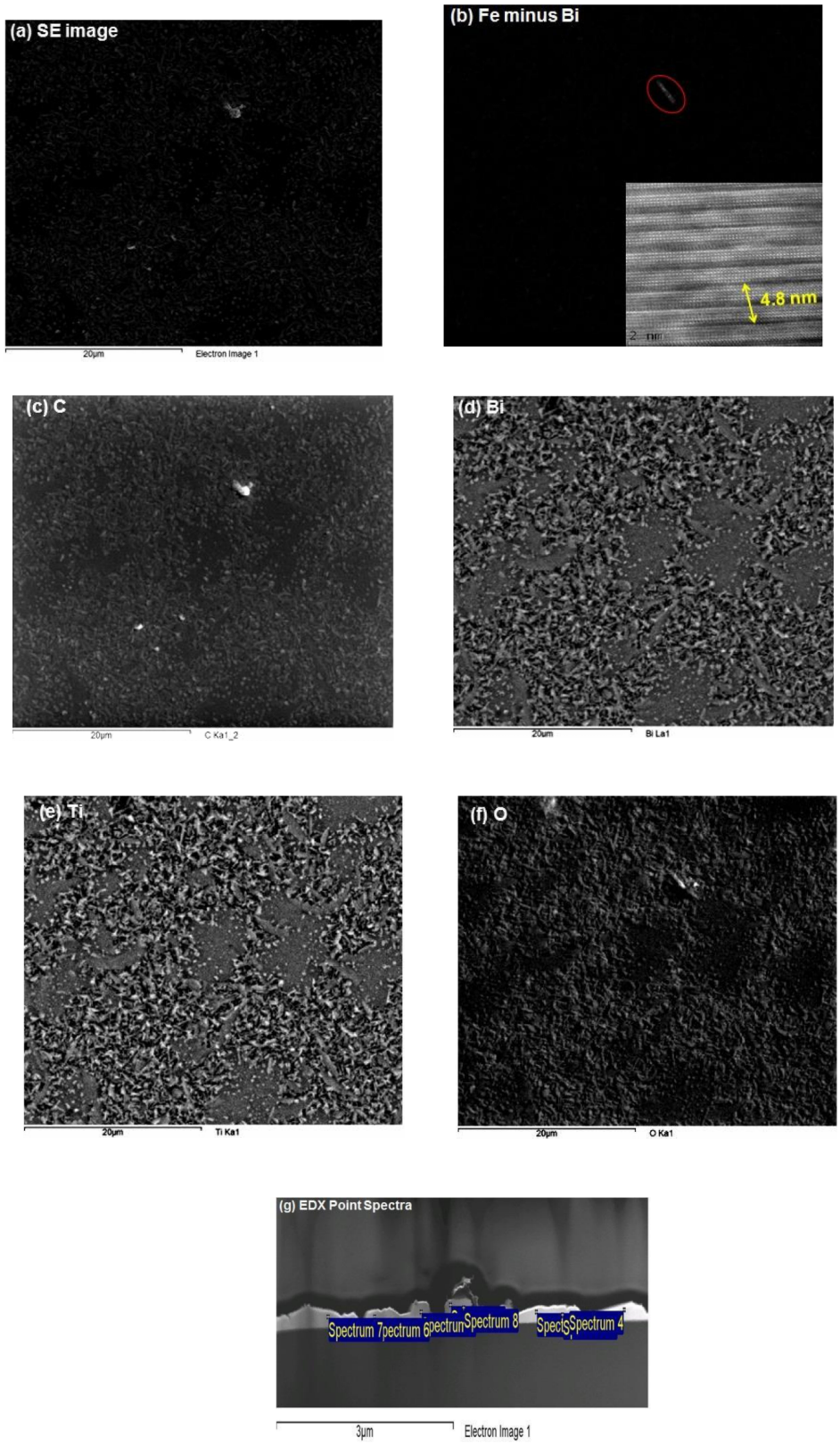

FIG. 4. Compositional analysis: Representative crossectional EDS map (51x44µm^2) of $Bi_6Ti_3Fe_2O_{18}$ on c-planer sapphir annealed at 850^{0}C for 10min (a) secondary electron image (b) Fe minus Bi distribution and HR-TEM of Fe rich area (inset) (c-f) elemental distribution (g) EDX point spectra.

All article content, except where otherwise noted, is licensed under a Creative Commons Attribution 3.0 Unported license. See: http://creativecommons.org/licenses/by/3.0/ Downloaded to IP: 143.239.65.133 On: Tue, 15 Sep 2015 07:37:49

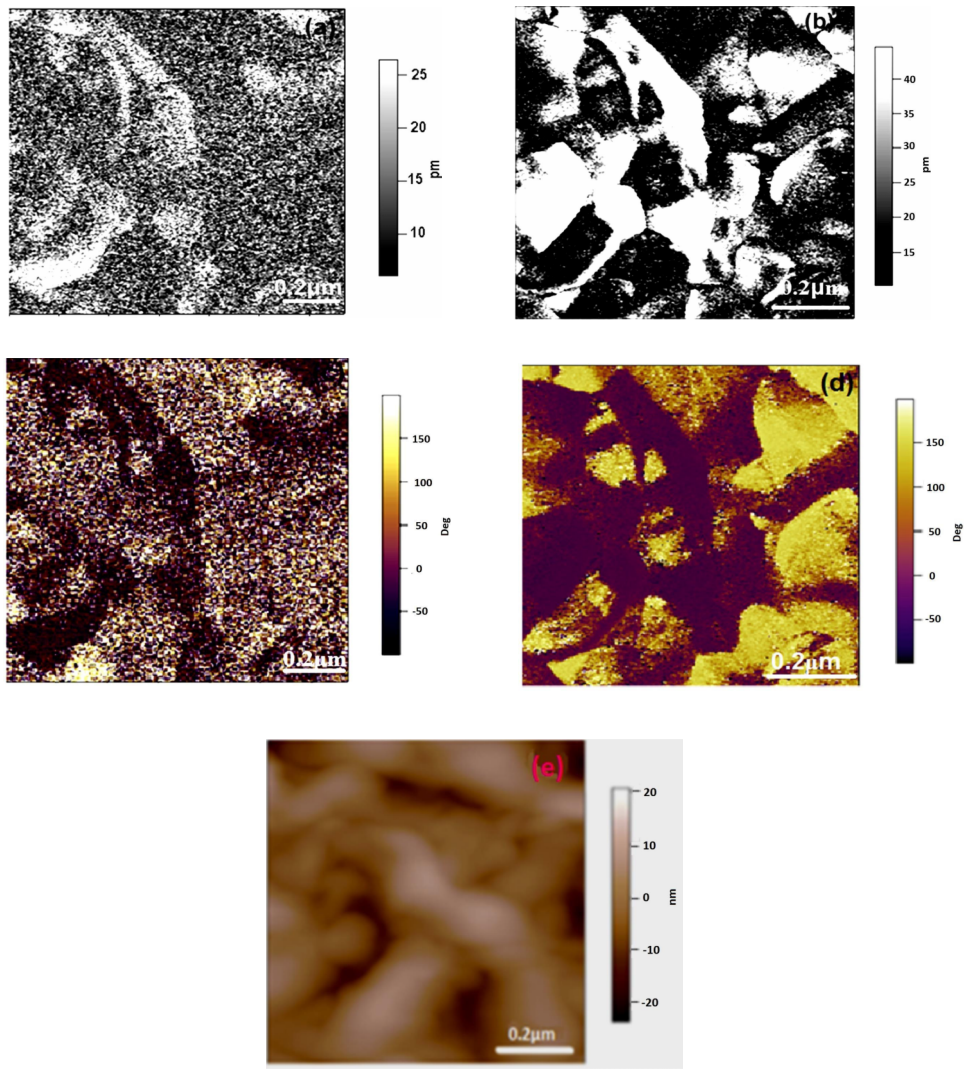

FIG. 5. Single frequency piezoresponse force microscopy micrographs for $B_6Ti_3Fe_2O_{18}$ m=5 layer thin films: (a) out-of-plane amplitude response (b) in-plane amplitude response (c) out-of-plane phase response (d) in-plane phase response (e) topography.

The potential of B6TFO for out-of-plane switching was further investigated by assessing vertical local electromechanical polarization and ferroelectric responses using the DART-vertical piezoresponse force microscopy (DART-VPFM) mode at room temperature.[30] This technique amplifies the out-of-plane polarization response in the Aurivillius phase thin films by enhancing the weaker vertical response signal. In DART-VPFM, the electrilever is sinusoidally excited near or at contact resonance frequency (300-310 kHz) to boost the electromechanical signal along the out-of-plane *c*-axis (vertical direction). Topographical cross talk and scanning artefacts in the DART-VPFM mode are reduced by contact resonance frequency tracking based on amplitude detection feedback.[30] Figure6(a)-6(c) shows representative vertical DART-VPFM micrographs of the polycrystalline B6TFO thin films. These micrographs illustrate the room temperature out-of-plane amplified amplitude and phase response signals from the minor polarization vector along the *c*-axis. The amplitude contrast (figure 6(b)) demonstrates the magnitude of the vertical piezoresponse, which is appreciable for B6TFO in this amplified PFM mode. Self-polarized multi-domains are clearly observable by comparing the topography image with phase and amplitude images. The image illustrates some domains with natural 180° polarization (c^+) which are the result of out-of-phase

All article content, except where otherwise noted, is licensed under a Creative Commons Attribution 3.0 Unported license. See: http://creativecommons.org/licenses/by/3.0/ Downloaded to IP: 143.239.65.133 On: Tue, 15 Sep 2015 07:37:49

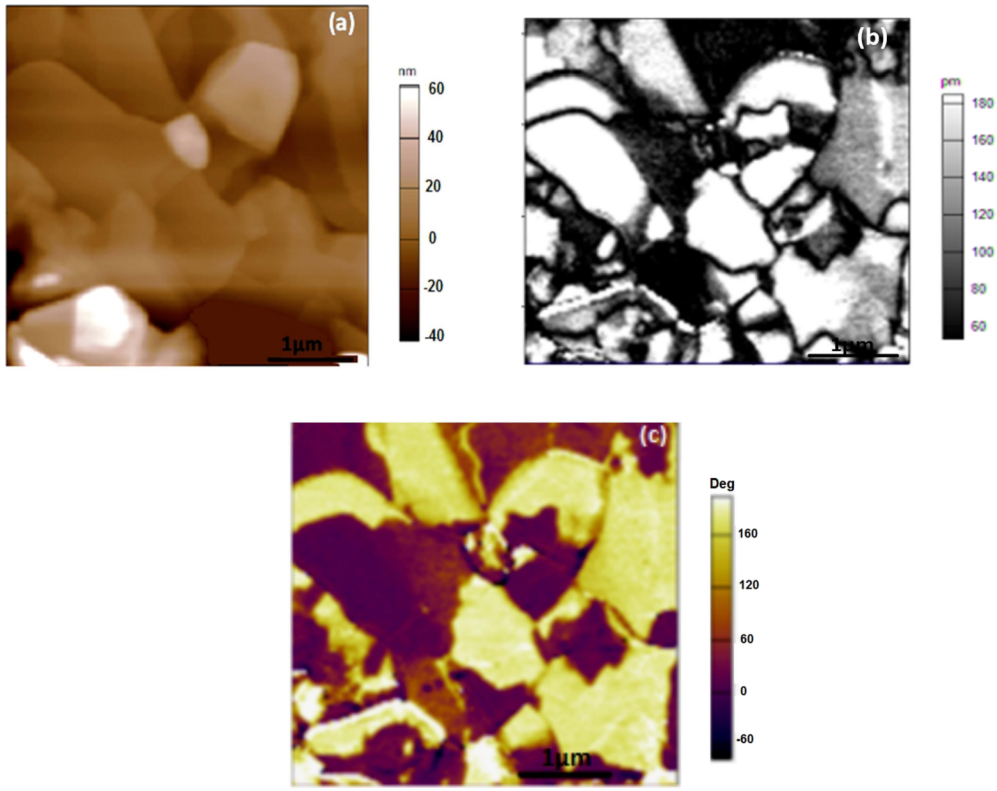

FIG. 6. Dual AC Resonance Tracking (DART) PFM amplified images of $Bi_6Fe_2Ti_3O_{18}$ (B6FTO) m=5 on sapphire substrate: (a) Height response (b) PFM amplitude response (c) PFM phase response.

local contraction of the sample under the influence of the ac tip bias, while the domains with 0° polarization (c^-) orientation are attributed to out-of-plane local expansion of the sample. A component of the out-of-plane electromechanical response (illustrated in figure 6(a)-6(c)) may also be attributed to some tilted, *a* or *b*-axis oriented grains which are accessible to probing in the vertical PFM mode. The difference between oppositely orientated (normal out-plane to the surface pointing downward or upward) domains is 180°.

2. Effect of temperature and applied bias (V_{dc}) on the ferroelectric switching properties

The 180° out-of-plane local electric field (V_{dc}) induced dipole reversibilty (ferroelectric polarization) and domain switching behavior in B6TFO thin films was investigated at room and elevated temperature (200°C) using DART switching spectroscopy PFM (DART-SSPFM) in the presence and absence of an applied DC-bias (Vdc), as represented by the hysteresis loops in figure 7. These loops clearly demonstrate the ferroelectric character of the B6TFMO thin films. While macroscopic hysteresis behavior involves nucleation and domain growth as a result of accumulation of multi-domains, in the case of PFM, local hysteresis involves the growth and nucleation of a single domain beneath the PFM tip.[32] Figure 6 represents an overview of domain growth, nucleation, switching and saturation in the B6TFO thin films at room temperature with an applied external DC field using the conducting PFM tip.

For clarity, the effect of applied bias (V_{dc}) at room temperature on domain switching, ferroelectric polarization reversal and saturation (P_s) are represented by generating hysteresis loops at different (40-60V) applied bias (V_{dc}) as illustrated in figure 7(a), where it was observed that the piezoelectric response increases with an increase in applied field (Vdc) until ferroelectric saturation (Ps) at 60V. 180° ferroelectric switching is clearly observed in the films (figure 7(b)) with a maximum observed vertical response of ~8 pm/V (figure 7(a)) and coercivity of 20V at room

All article content, except where otherwise noted, is licensed under a Creative Commons Attribution 3.0 Unported license. See: http://creativecommons.org/licenses/by/3.0/ Downloaded to IP: 143.239.65.133 On: Tue, 15 Sep 2015 07:37:49

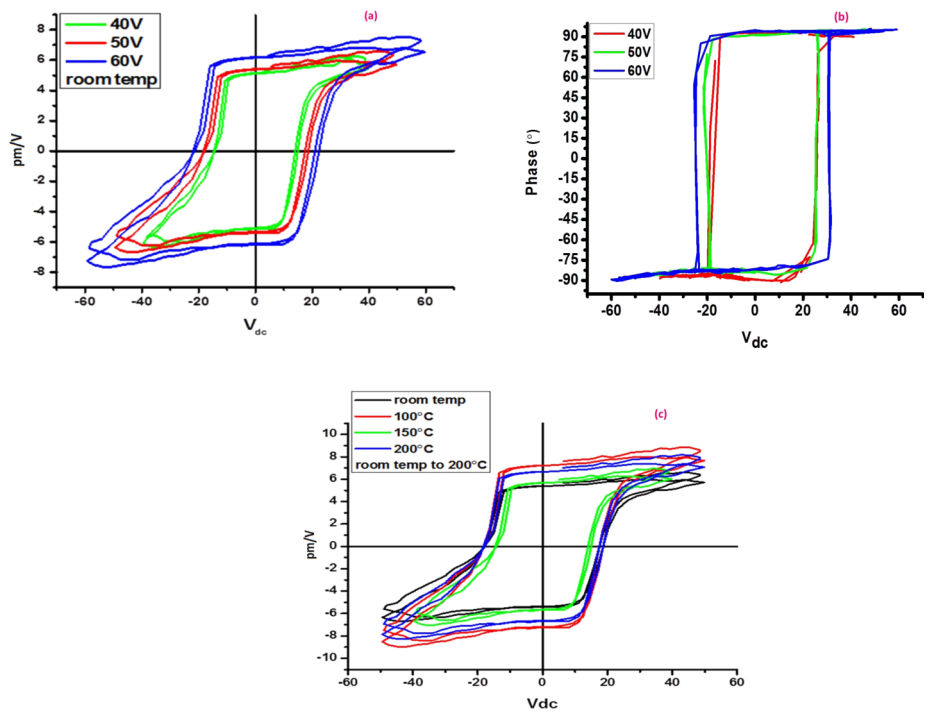

FIG. 7. Ferroelectric polarization switching with respect to applied external bias (V_{dc}): (a) Effect of bias on the magnitude of out-of-plane electromechanical (pm/V) response (b) Phase response with respect to applied bias. (c) Effect of temperature on the local out-of-plane electromechanical response.

temperature. The polarization reversal observed along the vertical direction is atributed to the minor c-axis polarization component characteristic of Aurivillius phase materials containing odd numbers of pervoskite units in their structure.

The increase in piezoelectric response observed with applied bias (V_{dc}) is attributed to domain growth in the expense of higher applied biases (V_{dc}). The phase response with respect to applied bias (V_{dc}) is represented in figure 7(b), where clear evidence of 180° ferroelectric switching is presented. The local ferroelectric switching in B6TFO thin films with respect to temperature is illustrated by comparing locally generated hysteresis loops generated at different tempreatures (room temperature to 200°C) represented by figure 7(c) where, it can be observed that polarization saturation (P_s), coercive field (H_c) and remanent polarization (P_r) increases with increasing temperature up to 200°C . This slight increase may be attributed to removal of surface residues at higher temperatures such as evaporation or removal of water molecules from the film surface. Small changes in piezoresponse of this nature with respect to increasing temperature demonstrates the stability of the ferroelectric properties of B6TFO up to 200°C and suggests that B6TFO thin films could be utilized for elevated temperature devices applications.[3,32]

3. Polarization switching by PFM lithography

The potential of B6TFO as a material for ferroelectric random access memory (Fe-RAMs) type applications depends on its ability to retain permement ferroelectric polarization at room and high temperature., because the binary codes in FeRAMs are asscoiated with up and down states of ferroelectric polarization.[36,38]

Ferroelectric polarization reversal depends on the minmum coercive field (H_c) required to switch the ferroelectric domains. A slightly higher field (70V) than the coercive field was applied to the B6TFO thin film in a writing step to ensure alignment of the polarization patterns along one direction. The quality of B6TFO thin films to retain polarization with respect to time and temperature was assessed on the basis of the DART-VPFM ferroelectric lithography technique

All article content, except where otherwise noted, is licensed under a Creative Commons Attribution 3.0 Unported license. See: http://creativecommons.org/licenses/by/3.0/ Downloaded to IP: 143.239.65.133 On: Tue, 15 Sep 2015 07:37:49

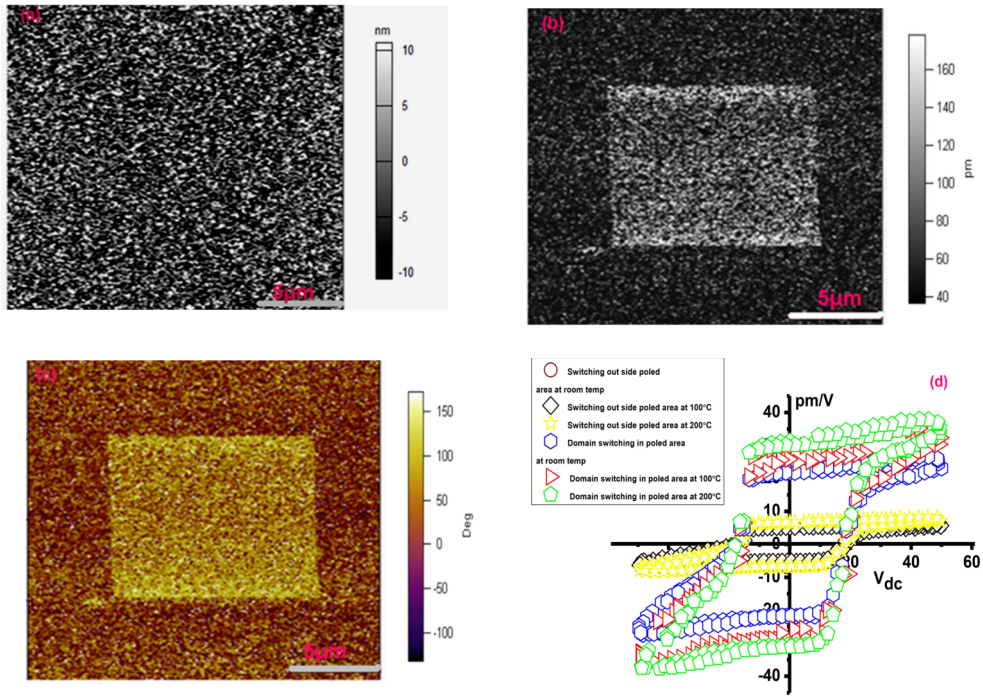

FIG. 8. Representative DART-VPFM images (scan size 20 $\mu m^2 \times 20 \mu m^2$) of B6TFMO thin films and comparison between domain orientation within a poled area (14 $\mu m^2 \times 14 \mu m^2$; 60V (Vdc) polarization field) and the surrounding un-poled area at 200ºC after 20hrs in the reading step: (a) surface topography, (b) amplitude image demonstrating out-of-plane piezoresponse (c) phase image demonstrating the direction of the written domain pattern. (d) DART SSPFM hysteresis loops showing comparisons between the magnitude of domain switching within the polled (14x14 μm^2) areas and the outside un-polled areas at room and elevated temperatures.

which involves writing and reading multi-domain patterns or arrays without any topographical changes to the sample surface.[30] This technique was used to exploit the ferroelectric polarization along the *c*-axis in the B6TFO thin films. Ferroelectric lithography was performed on an area 20x20 μm^2 and 130 nm thick B6TFO thin film with respect to temperature (200°C) as represented by Figure 8(a)-8(c). Within this area, a square type box of area 14x14 μm^2 was poled during the lithography 'write' step by applying a 60V DC field (V_{dc}) (higher than the coercive field of 20V)) vertically to the surface of B6TFO thin films at 200^0C. This higher applied direct field (V_{dc}) causes ferroelectric polarization switching and re-orientation of the ferroelectric dipoles along the upward direction over the polarized square area (14x14μm^2) in the PFM 'writing' step.[32,33,37,38] The 'written' scanned area (at 200°C) was further scanned over 20hrs in the normal DART-VPFM mode while the sample stage was maintained at a temperature of 200°C and same written patterns remained over this time as detected in the 'reading step' (figure8(a)-8(c)), confirming that B6TFO thin film retains polarization over this finite period of time at this higher temperature.

Ferroelectric polarization switching behavior was quantitatively assessed by generating hysteresis loops with respect to applied bias (Vdc) within the written domain square pattern at room and high temperatures after 20hrs of poling the 14 x 14 μm^2 area, as is illustrated in figure 8(d). From this figure it can be observed that the hysteresis loops generated from the poled regions demonstrate significantly higher vertical piezoresponses (25 pm/V) compared with the unpoled areas outside the 14 x 14 μm^2 square (~8pm/V) (figure 8(d)). The higher piezoresponses observed may be attributed due to the accumulative switching of polled domain arrays. Such accumulative polarization switching is attributed to the ferroelectric switching transient effect.[39,40] When a bias (V_{dc}) is applied from the PFM tip, this results in dielectric polarization followed by polarization reversal. If the applied field (V_{dc}-on) is turned off before completion of polarization reversal, this may result in depolarization of the dielectric polarization of each component of the switched ferroelectric domain and effected neighbor ferroelectric domains with their inherent decay time.[40]

All article content, except where otherwise noted, is licensed under a Creative Commons Attribution 3.0 Unported license. See: http://creativecommons.org/licenses/by/3.0/ Downloaded to IP: 143.239.65.133 On: Tue, 15 Sep 2015 07:37:49

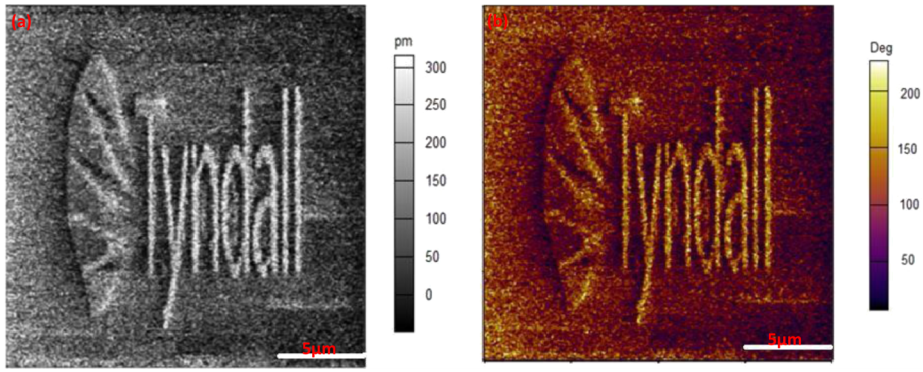

FIG. 9. PFM image of fine ferroelectric domain features (a) written in the B6Ti3Fe2O18 thin films using PFM lithography with an applied DC bias of Vdc = 70V at 200°C and (b) read after 20hrs at 200ºC. This data confirms the stability of the fine ferroelectric polarization patterns and the potential use of B6Ti3Fe2O18 in high data storage technologies. The typical domain widths are 100-300nm.

Furthermore, the effect of temperature on the piezoresponse in the poled area and comparison between the piezoresponse observed from un-poled domains and within the poled area is illustrated in figure 8(d). It can be observed that remnant polarization (P_r) and saturation polarization (P_s) increases slightly with increase in temperature in both cases, most likely due to the loss of surface residues e.g. water at higher temperature.

High density ferroelectric data storage media are typically associated with fine feature sizes with increased polarization magnitudes which can be encoded into at least two directions/states of binary code. In the case of the B6TFO thin films, polarization patterns with typical domain width of 100-300nm were easily introduced and written at an applied bias of 70V. The stability of retaining polarization patterns were observed on removal of the applied bias (V_{dc}) in the 'read step' as illustrated by figure 9(a)-9(b). It should be noted that the fine pattern was written at 200°C and read after 20hr at the same temperature, confirming ferroelectric polarization stability of fine B6TFO patterns up to this finite period of time and are stable at elevated temperatures (200°C). The stability of the ferroelectric polarization pattern with respect to time and temperature suggests the suitabilty of this ferroelectric material for potential application as active components in non-volatile memory devices (FeRAM) at room and higher temperatures.

IV. CONCLUSIONS

In summary, highly textured B6TFO thin films containing five perovskite units (n=5) per half unit cell were grown on c-axis oriented sapphire substrates by a liquid injection chemical vapor deposition process (LI-CVD) using dilute liquid precursors. Microstructural annalysis demonstrated that B6TFO thin films annealed at 850°C for 10 minutes are 5-layered Aurivillius phases with no additional detectable secondary impurity phases. PFM results establish that the B6TFO thin films are piezoelectric and ferroelectric at room temperature with the major polarization vector component in the lateral plane (a-axis) of the films. There was no decrease in the switching polarization and saturation (P_s) piezoresponse with increasing temperature (200°C) for the B6TFO thin films, demonstrating the stability of the films at elevated temperature and applied bias. Poled areas and fine domain patterns (typical domain width 300nm) are stable with respect to temperature up to 200°C and the films retain polarization for a period of at least 20hrs. The B6TFO films demonstrate potential for possible future commercial applications in high temperature piezoelectric sensing applications since they are lead free piezoelectrics exhibiting switching between two stable polarization states at elevated temperatures. The ability of B6TFO to store ferroelectric polarization, at room and high temperatures, makes it a potential candidate for memory storage devices which are stable at elevated temperature.

All article content, except where otherwise noted, is licensed under a Creative Commons Attribution 3.0 Unported license. See: http://creativecommons.org/licenses/by/3.0/ Downloaded to IP: 143.239.65.133 On: Tue, 15 Sep 2015 07:37:49

ACKNOWLEDGMENTS

The support of Science Foundation Ireland (SFI) under the FORME Strategic Research Cluster Award number 07/SRC/I1172, the Irish Higher Education Authority (HEA) PRTLI 3, HEA PRTLI4 Project INSPIRE and the support of the 7th Framework Programme Marie Curie Initial Training Network under the NANOMOTION Grant agreement no.: 290158 is gratefully acknowledged. This publication has emanated from research conducted with the financial support of Science Foundation Ireland under Grant "SFI 13/TIDA/I2728".

[1] R. E. Cohen, "Origin of ferroelectricity in perovskite oxides," Nature **358**, 136-138 (1992).
[2] P. Ferreira, R.Z Hou, A. Wu, M.G Willinger, P.M Vilarinho, J. Mosa, C. Robert, C. Boissière, D. Grosso, and C. Sanchez, "Nanoporous piezo- and ferroelectric thin films," Lang. **28**, 2944–2949 (2012).
[3] H. T. Y. Saito, T. Tani, T. Nonoyama, K. Takatori, T. Homma, T. Nagaya, and M. Nakamura, "Lead-free piezoceramics," Nature **432**, 84-87 (2004).
[4] E. Y. Tsymbal and A. Gruverman, "Ferroelectric tunnel junctions: Beyond the barrier," Nature materials **12**, 602–604 (2013).
[5] M. Bibes and A. Barthélémy, "Multiferroics: Towards a magnetoelectric memory," Nature materials **7**, 425-426 (2008).
[6] B. Jaffe, R. S. Roth, and S. Marzullo, "Piezoelectric Properties of Lead Zirconate-Lead Titanate Solid-Solution Ceramics," Res. Natl. Bur. Stand. **55**(5), 239-252 (1955).
[7] Y. Fukuda, M. Pecht, K. Fukuda, and S. Fukuda, IEEE Transactions on Components and Packaging Technologies **26**, 616-624 (2003).
[8] P. Casey and M. Pecht, IPC/JEDEC International Conference on Lead-Free Electronic Components and Assemblies, 21-32 (2002).
[9] H. Nagata, M. Yoshida, Y. Makiuchi, and T. Takenaka, "Large Piezoelectric Constant and High Curie Temperature of Lead-Free Piezoelectric Ceramic Ternary System Based on Bismuth Sodium Titanate-Bismuth Potassium Titanate-Barium Titanate near the Morphotropic Phase Boundary," Jpn. J. Appl. Phys **42**(12R), 7401 (2003).
[10] J. C. Bae, S. Kim, E. K. Choi, T. K. Song, W. J. Kim, and Y. I Lee, "Ferroelectric properties of lanthanum-doped bismuth titanate thin films grown by a sol–gel method," Thin. Sol. Films **472**, 90–95 (2005).
[11] A. Duk, J. Schwarzkopf, A. Kwasniewski, M. Schmidbauer, and R. Fornari, "Impact of crystallographic structure expetexially grown Sodium-Bismuth-Titanate thin films on Local Piezo and Ferroelectric properties," Mat.Res.Bull. **47**, 2056–2061 (2012).
[12] F. Sugawara, S. Iida, Y. Syono, and S. Akimoto, "Magnetic Properties and Crystal Distortions of BiMnO3 and BiCrO3," Phys.Soc. Jpn **25**, 1553 (1968).
[13] T. Atou, H. Chiba, K. Ohoyama, Y. Yamaguchi, and Y. Syono, "Structure determination of ferromagnetic perovskite BiMnO3," Sol. Stat. Chem **145**, 064425-064424 (2002).
[14] P. Baettig, C. F. Schelle, R. LeSar, U. V. Waghmare, and N. A. Spaldin, "Theoretical Prediction of New High-Performance Lead-Free Piezoelectrics," Chem. Mater **17**, 1376-1380 (2005).
[15] B. Aurivilius and P. H. Fang, "Ferroelectricity in the Compound Ba2Bi4Ti5O1," Phys.Rev **126**(3), 893-897 (1962).
[16] Z. Liu, J. Yang, X. W. Tang, L. H. Yin, X. B. Zhu, J. M. Dai, and Y. P. Sun, "Multiferroic properties of Aurivillius phase Bi 6 Fe 2-x Co x Ti 3 O 18 thin films prepared by a chemical solution deposition route," App.Phys.Lett **101**, 122402-122404 (2012).
[17] L. Keeney, T. Maity, M. Schmidt, A. Amann, N. Deepak, N. Petkov, S. Roy, M.E. Pemble, and R.W. Whatmore, "Magnetic Field-Induced Ferroelectric Switching in Multiferroic Aurivillius Phase Thin Films at Room Temperature," Am. Ceram. Soc. **96**(8), 2339–2357 (2013).
[18] N. A. Lomanova, M. I. Morozov, V. L. Ugolkov, and V. V. Gusarov, "Properties of aurivillius phases in the Bi4Ti3O12-BiFeO3 system," Inorg. Mater **42**(2), 189–195 (2006).
[19] W. C Tzou, K. H Chen, C. F Yang, and T. L Tsai, Ferroelectrics **385**(1), 654-661 (2009).
[20] P. Gautam, S. Bhattacharyya, S. K. Singh, and R. P. Tandon, "Memory Properties of SrBi2Ta2O9 Ferroelectric Thin Film Prepared on SiO2/Si Substrate," Integ. Ferroelectrics **122**(1), 63-73 (2010).
[21] B. H. Park, B. S. Kang, S. D. Bu, T. W. Noh, J. Lee, and W. Jo, "Lanthanum-substituted bismuth titanate for use in non-volatile memories," NATURE **401**, 682-684 (1999).
[22] P. F. Zhang, N. Deepak, L. Keeney, M. E. Pemble, and R. W. Whatmore, "The structural and piezoresponse properties of c-axis-oriented Aurivillius phase Bi5Ti3FeO15 thin films deposited by atomic vapor deposition," Appl. Phys. Lett. **101**, 112903-112904 (2012).
[23] L. Keeney, C. Groh, S. Kulkarni, S. Roy, M. E. Pemble, and R. W. Whatmore, "Room temperature electromechanical and magnetic investigations of ferroelectric Aurivillius phase Bi5Ti3 (FexMn1- x) O15 (x = 1 and 0.7) chemical solution deposited thin films," Appl. Phys. **112**, 024101-024109 (2012).
[24] A.T. Giddings, M.C. Stennett, D.P. Reid, E.E. McCabe, C. Greaves, and N.C. Hyatt, "Synthesis, structure and characterisation of the n1/44 Aurivillius phase Bi5Ti3CrO15," J. Sol. Stat. Chem. **184**, 252–263 (2011).
[25] M. A. Zurbuchen, N. J. Podraza, J. Schubert, Y. Jia, and D. G. Schlom, "Synthesis of the superlattice complex oxide Sr5Bi4Ti8O27 and its band gap behavior," Appl. Phys. Lett **100**, 223109-223104 (2012).
[26] N. Deepak, P. F. Zhang, L. Keeney, M. E. Pemble, and R. W. Whatmore, "Atomic vapor deposition of bismuth titanate thin films," Appl. Phys **113**, 187207-187207 (2013).
[27] R. Furushima, S. Tanaka, Z. KATO, and K. Uematsu, "Orientation distribution–Lotgering factor relationship in a polycrystalline material—as an example of bismuth titanate prepared by a magnetic field," Cer. Soc. Jpn **118**(10), 921-926 (2010).
[28] Crystallographica - a software toolkit for crystallography, Appl. Cryst 30, 418–419 (1997).
[29] E. Soergel, "Piezoresponse force microscopy (PFM)," D: Appl. Phys **44**, 464003 (2011).
[30] B. J. Rodriguez, C. Callahan, S. V. Kalinin, and R. Proksch, "Dual-Frequency Resonance-Tracking Atomic Force Microscopy," Nanotechnology **18**(47), 475504-475506 (2007).

All article content, except where otherwise noted, is licensed under a Creative Commons Attribution 3.0 Unported license. See: http://creativecommons.org/licenses/by/3.0/ Downloaded to IP: 143.239.65.133 On: Tue, 15 Sep 2015 07:37:49

[31] L. Keeney, S. Kulkarni, N. Deepak, M. Schmidt, N. Petkov, P. F. Zhang, S. Cavill, S. Roy, M. E. Pemble, and R. W. Whatmore, "Room temperature ferroelectric and magnetic investigations and detailed phase analysis of Aurivillius phase Bi5Ti3Fe0. 7Co0. 3O15 thin films," J. Appl. Phys **112**, 052010-10 (2012).
[32] S. Jesse, A. P. Baddorf, and S.V. Kalinin, "Switching spectroscopy piezoresponse force microscopy of ferroelectric materials," Apps. Phys. Lett **88**, 062908-062903 (2006).
[33] A. Gruverman and S. V. Kalinin, "Piezoresponse force microscopy and recent advances in nanoscale studies of ferroelectrics," Mat.Sci **41**, 107–116 (2006).
[34] S. V. Kalinin, A. Gruverman, B. J. Rodriguez, J. Shin, A. P. Baddorf, E. Karapetian, and M. Kachanov, "Nanoelectromechanics of polarization switching in piezoresponse force microscopy," Appl. Phys **97**, 074305-074306.
[35] R. E. Newnham, R. W. Wolfe, and J. F. Dorrian, "Structure basis of ferroelectricity in the bismuth titanate family," Mat. Res. Bull **6**, 1029-1040 (1971).
[36] K. Kim and Y. J. Song, "Integration technology for ferroelectric memory devices," Micro. Rel. **43**(3), 385–398 (2003).
[37] V. Garcia, "Manuel Bibes, Electronics: Inside story of ferroelectric memories," NATURE **483**, 279–281 (2012).
[38] F. Yang, Y.C Zhou, M.H Tang, F. Liu, Y. Ma, X.J Zheng, W.F Zhao, H.Y Xu, and Z.H Sun, "Eight-logic memory cell based on multiferroic junctions," Phys. D: Appl. Phys **42**, 072004 (072006pp) (2009).
[39] M. Nishino, C. Enachescu, S. Miyashita, P. A. Rikvold, K. Boukheddaden, and F. Varret, "Macroscopic nucleation phenomena in continuum media with long-range interactions," Sci. Rep. **1**, 162 (2011).
[40] J.Y. Jo, H. S. Han, J.G. Yoon, T. K. Song, S.H. Kim, and T.W. Noh, "Domain switching kinetics in disordered ferroelectric thin films," Phy.Rev.Lett **99**, 267602-267604 (2007).

All article content, except where otherwise noted, is licensed under a Creative Commons Attribution 3.0 Unported license. See: http://creativecommons.org/licenses/by/3.0/ Downloaded to IP: 143.239.65.133 On: Tue, 15 Sep 2015 07:37:49